

Adsorption of Iron and Manganese Ions from Mine Acid Water Using Manganese Green Sand in Batch Process

Esthi Kusdarini^{1*}, Putri Rizka Sania¹, Agus Budianto²

¹ Mining Engineering Department, Adhi Tama Institute of Technology Surabaya, Jl. Arief Rachman Hakim 100 Surabaya 60117, Indonesia

² Chemical Engineering Department, Adhi Tama Institute of Technology Surabaya, Jl. Arief Rachman Hakim 100 Surabaya 60117, Indonesia

* Corresponding author's e-mail: esti@itats.ac.id

ABSTRACT

Fe and Mn metal ions in acid mine drainage can contaminate water bodies and soil, endangering human health. In this study, the adsorption of Fe and Mn in acid mine drainage was carried out using manganese greensand. This study aimed to obtain 1) the adsorption model of Fe and Mn isotherms using manganese greensand and 2) the surface morphology of manganese greensand before and after the adsorption process. This study used laboratory-scale experimental methods with variable concentrations of Fe (325, 400, 475, 550, 625 mg/L) and Mn (432, 507, 582, 657, 732 mg/L). The Freundlich and Langmuir adsorption isotherm models were used to determine the adsorption capacity of Fe and Mn by manganese greensand. Test for Fe and Mn content using the AAS method and test the surface morphology and content of manganese greensand using SEM-EDX. The results showed that: (1) the Freundlich equation test yielded for Fe: in a constant R^2 of 0.9862, $n = 0.6912$, $KB = 0.2180$ mg/g, while the Langmuir equation test yielded in a constant R^2 of 0.8836, $b = 0.0051$ L/mg, $q_m = 169.4915$ mg/g; the Freundlich equation test yielded for Mn: in a constant R^2 of 0.9923, $n = 0.8651$, $KB = 1.0445$ mg/g, while the Langmuir equation test yielded in a constant R^2 of 0.6615, $b = 0.0010$ L/mg, $q_m = 500$ mg/g; (2) The surface morphology of manganese greensand before contact with acid mine drainage contains needle-shaped particles of uniform size with a hexagonal structure, whereas, after contact with acid mine drainage, the particles are clumped like cotton and form needles with varying sizes.

Keywords: adsorption, batch process, iron, manganese greensand, mine acid water

INTRODUCTION

The mining process of mineral ores containing sulfur has the potential to form acid mine drainage. Acid mine drainage is acidic and can potentially contain heavy metals that harm human health and the sustainability of the surrounding environment. The pH of acid mine water ranges from 3 to 6. Several heavy metals that are often found in acid mine water are Fe, Mn, and Al (Gautama, 2019). Ogugua et al. also found that acid mine water used to water tomato plants resulted in Cd, Cr, Cu, Ni, and Zn metals accumulation in roots, stems, and leaves (Ogugua et al., 2022). Acid mine drainage contaminates groundwater and causes groundwater to contain SO_4 , Zn, and Tl

(Jung et al., 2023). The content of heavy metals in acid mine drainage can endanger human health.

Tehrani et al. found that the soil near the waste rock pile contains As, Cd, Pb, Ni, and Zn. Miners' average blood levels of Zn, Pb, and Cd exceed safe concentrations for adults, while 30% of workers tested positive for As in the blood (Tehrani et al., 2023). Belle et al. also found that gold mining in the Welkom and Virginia regions of the Free State Province of South Africa has generated large amounts of gold mine tailings, which contain various contaminants. These pollutants cause groundwater contamination with the dominant toxic metals, namely Fe and Pb (Belle et al., 2021). Several studies have been conducted

to overcome heavy metal pollution in general industrial wastewater and the mining industry.

The research to reduce the heavy metal content in polluted water is carried out using several treatment methods, including filtration (Kusdarini et al., 2021; Kusdarini et al., 2019; Kusdarini et al., 2020), adsorption (Budianto et al., 2021; Budianto et al., 2021; Budianto et al., 2019; Budianto et al., 2023; Kusdarini et al., 2022), ion exchanger (Kusdarini & Budianto, 2018; Kusdarini et al., 2018; Kusdarini et al., 2021; Kusdarini et al., 2017; Kusdarini et al., 2018).

These studies have resulted in findings on reducing the content of several heavy metals, including Fe and Mn, by up to 99%; however, the operational costs and the processing techniques are quite complicated. This study complements the previous research by using manganese greensand adsorber, which is relatively cheap and can be washed to be used repeatedly. In addition, this study also developed a model of the Freundlich and Langmuir isothermic adsorption equation that was obtained. Therefore, this research is highly important in order to obtain the information on the adsorption capacity of manganese greensand on the Fe and Mn metals contained in acid mine drainage.

MATERIALS AND METHODS

Materials and tools

The materials used in this study were samples of acid mine drainage (taken from the coal mining area of PT. X in East Kalimantan, Indonesia), manganese greensand, FeSO_4 , MnCl_2 and distilled water. The tools used are: analytical balance, filter paper, furnace, beaker glass, aluminium foil, funnel, measuring cup, stirrer, and Erlenmeyer flask.

Experimental procedure

The experiment was divided into five stages: 1) preparing 20 samples of modified acid mine drainage (200 mL each) into a beaker glass; 1a) modification of the Fe content of samples A: 375, B: 450, C: 525, D: 600, E: 675 mg/L; 1b) modification of the Mn content of samples F: 432, G: 507, H: 582, I: 657, J: 732 mg/L; 2) adding 0.2 gram of manganese green sand into each beaker glass and stirring at 150 rpm for 4 hours; 2) analysis of the Fe content in samples A, B, C, D,

E and the Mn content in samples F, G, H, I, J using the atomic absorption spectroscopy method (SNI 6989.71:2009); 4) Morphological analysis of manganese greensand before and after contact with acid mine drainage using SEM-EDX.

Adsorption isotherm model analysis

The adsorption isotherm model investigation was carried out using the Freundlich and Langmuir equations. Freundlich postulated the existence of heterogeneous surfaces with varying adsorption energies; as per Equation (6), KB and n represent the Freundlich constants that define the adsorption capacity and intensity. These constants can be determined from the intercept and slope of the logarithmic plot of q_e versus C_e (Nowruzzi et al., 2020).

$$q_e = KB C_e^{\frac{1}{n}} \quad (6)$$

The q_e notation represents the equilibrium capacity of metal ions, denoting the quantity of metal ions adsorbed per unit mass of green sand (mg/g). C_e represents the equilibrium concentration of metal ions in the solution after activated carbon adsorption (mg/L). KB and n are empirical constants (Basu et al., 2018; Kusdarini et al., 2018, 2021). The KB and n constants can be found in Equation (7).

$$\log q_e = \log KB + \frac{1}{n} \log C_e \quad (7)$$

Determining the KB and n constants of Freundlich Equation was done by plotting $\log q_e$ vs $\log C_e$ as in Equation (7). The Langmuir isothermal adsorption equation is represented by Equation (8).

$$\frac{C_e}{q_e} = \frac{C_e}{q_m} + \frac{1}{b q_m} \quad (8)$$

C_e (mg/L) represents the equilibrium concentration of metal ions in the solution following adsorption by green sand. q_e (mg/g) denotes the equilibrium capacity for metal ions, specifically the weight of metal ions adsorbed per unit weight of green sand. In turn, b (L/mg) and q_m (mg/g) represent the Langmuir constants, corresponding to the adsorption energy and the maximum adsorption capacity, respectively. These constants are determined from the intercept and slope of the C_e/q_e versus C_e diagram (Budianto et al., 2023).

RESULTS

This study revealed the adsorption capacity of Fe and Mn ions contained in acid mine drainage by manganese greensand. The mechanism of the adsorption process of Fe and Mn ions into greensand minerals is presented in Figure 1. Adsorptive Fe and Mn ions in acid mine water have the potential to be absorbed by greensand mineral adsorbents. Fe and Mn ions become adsorbates when the greensand minerals have adsorbed them. If the greensand minerals are not saturated, the adsorption process will continue, but if the greensand minerals are saturated, the speed of the adsorption process will be the same as the speed of the desorption process (re-release of Fe and Mn adsorbate ions into mine acid water).

Adsorption isothermic model analysis

The Freundlich and Langmuir adsorption isothermic model explains the adsorption process of the Fe and Mn ions contained in acid mine water. Data collection for initial Fe and Mn

concentrations and at equilibrium conditions is presented in Tables 1 and 2.

Furthermore, when it reaches an equilibrium condition, the greater the concentration of Fe and Mn contained in acid mine drainage, the lower the percentage of adsorption of Fe and Mn, as shown in Figure 2 (Fe adsorption) and Figure 3 (Mn adsorption).

Figure 2 shows that greensand can remove up to 69.94% Fe and up to 70.61% Mn, so its adsorption power is higher than activated carbon, which is only able to adsorb 53% (Kusdarini & Budianto, 2022; Kusdarini et al., 2022). The percentage of Fe and Mn removal by greensand produced in this study was also higher than that found by Galangashi et al., which was around 42% for Fe and 27% for Mn (Galangashi et al., 2021). This finding is consistent with previous findings, which explained that the purple-black manganese green sand material can adsorb Fe, Mn, As, and Ra due to its adsorbent and ion exchanger properties. This process occurs due to manganese coated with MnO₂ in greensand. Each glauconite grain has a limited amount of MnO₂. MnO₂ can increase the Mn content in zeolite from

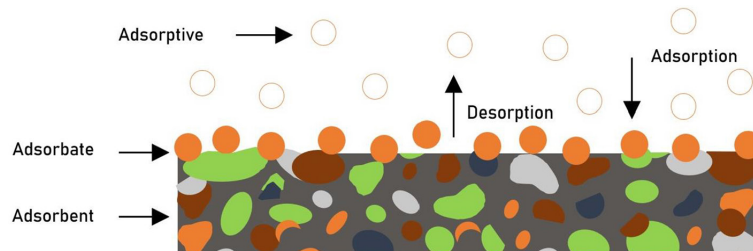


Figure 1. Adsorption mechanism

Table 1. Fe concentration for determining the Freundlich and Langmuir equations

Sample	C _o (mg/L)	C _e (mg/L)	q _e = C _o - C _t (mg/L)	%A	log C _e	log q _e	C _e /q _e
A	375	127.7	247.3	65.95	2.3073	2.6254	1.9366
B	450	152.2	297.8	66.18	2.2472	2.5721	1.9566
C	525	164.9	360.1	68.59	2.2172	2.5564	2.1837
D	600	183.4	416.6	69.43	2.2634	2.6197	2.2715
E	675	202.9	472.1	69.94	2.3073	2.6740	2.3268

Table 2. Mn concentration for the Freundlich and Langmuir equations

Sample	C _o (mg/L)	C _e (mg/L)	q _e = C _o - C _t (mg/L)	%A	log C _e	log q _e	C _e /q _e
F	432	135.1	296.9	68.73	2.1307	2.4726	2.1976
G	507	152.2	354.8	69.98	2.1824	2.5500	2.3311
H	582	172.2	409.8	70.41	2.2360	2.6126	2.3798
I	657	196.3	460.7	70.12	2.2929	2.6634	2.3469
J	732	215.1	516.9	70.61	2.3326	2.7134	2.4031

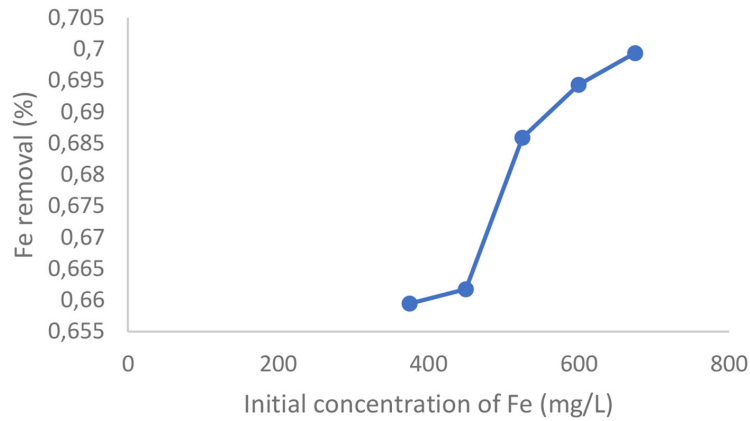


Figure 2. The effect of the initial concentration of Fe on the percentage of Fe adsorption

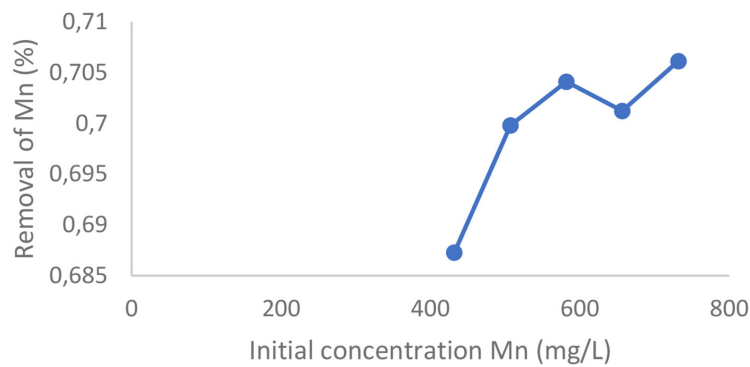


Figure 3. The effect of the initial concentration of Mn on the percentage of Mn adsorption

0.19% to 0.85%. In addition to the role of MnO_2 , which helps the deposition of metal ions, manganese green sand has pore dimensions of $0.45 \times 10^{-6} - 2.67 \times 10^{-6}$ mm, and the number of pores is quite large so that it can absorb particles with smaller sizes than pores (Outram et al., 2017).

Furthermore, the Fe ion adsorption process modeled by the Freundlich equation (Figure 4) is

better than the Langmuir equation (Figure 5). The R^2 value of the Freundlich equation is closer to 1 than the R^2 Langmuir equation. This trend also occurs in the Mn ion adsorption process, modeled by the Freundlich equation (Figure 6), which is better than the Langmuir equation (Figure 7).

The adsorption of Fe and Mn by greensand minerals is obtained, presented in Table 3.

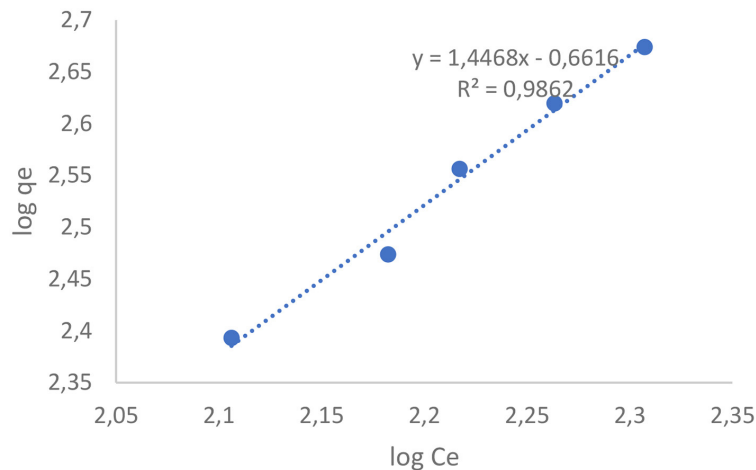


Figure 4. Freundlich adsorption isotherm model for Fe

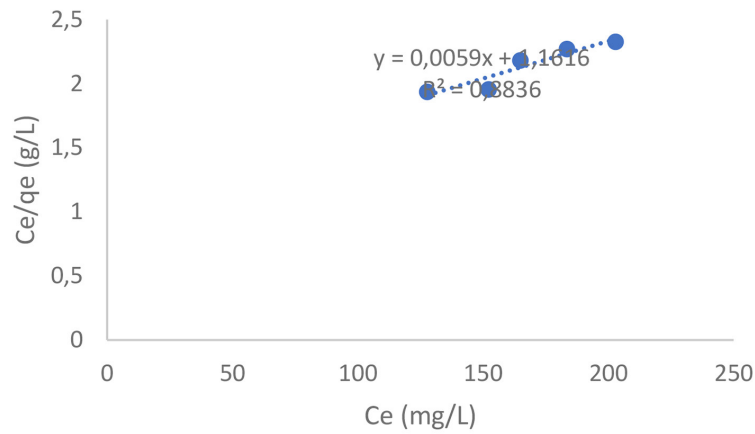


Figure 5. Langmuir adsorption isotherm model for Fe

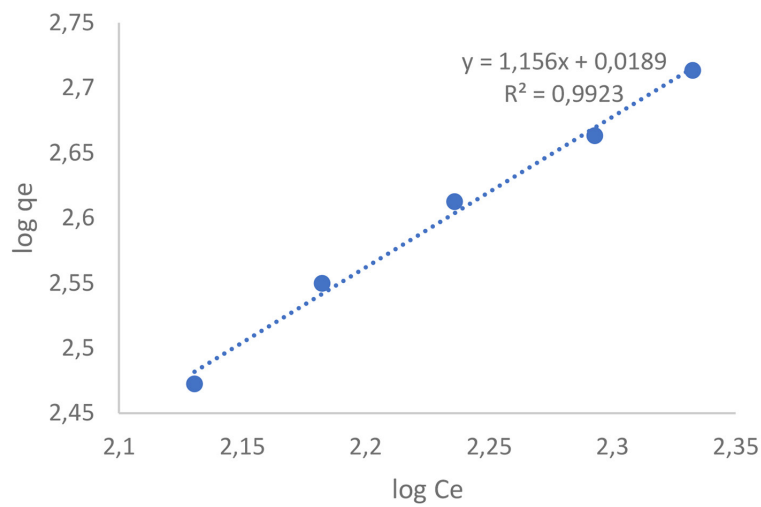


Figure 6. Freundlich adsorption isotherm model for Mn

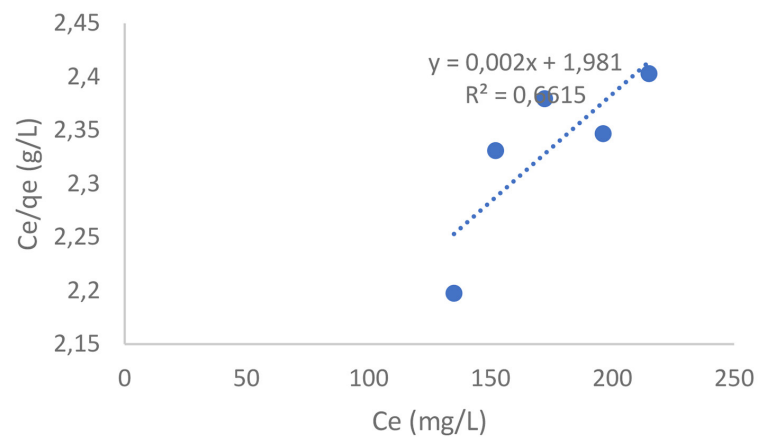


Figure 7. Langmuir adsorption isotherm model for Mn

EDX SEM analysis

The greensand surface morphology before and after the adsorption process of Fe and Mn is presented in Figure 8–11.

Figures 8 and 9 show that the morphology of manganese greensand before the adsorption process contains particles of uniform size, pointed like a needle, which causes a high crystallinity value. This particle is thought to be quartz mineral

Table 3. Freundlich and Langmuir equation constants

Adsorbate	Freundlich			Langmuir		
	R^2	n	KB (mg/g)	R^2	b (L/mg)	q_m (mg/g)
Fe	0.9862	0.6912	0.2180	0.8836	0.0051	169.4915
Mn	0.9923	0.8651	1.0444	0.6615	0.0010	500,0000

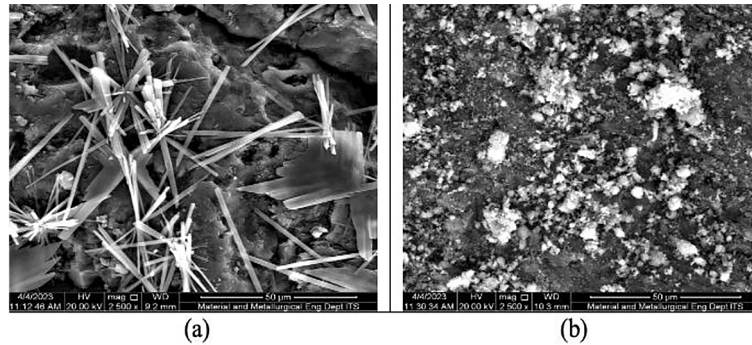


Figure 8. Morphology of green sand (1000×): (a) before adsorption, (b) after adsorption

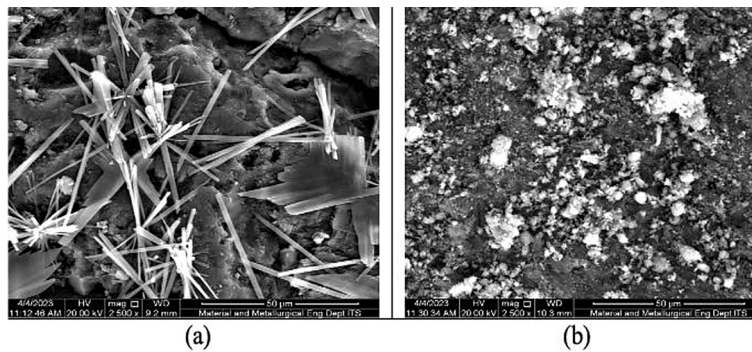


Figure 9. Morphology of green sand (2500×): (a) before adsorption, (b) after adsorption

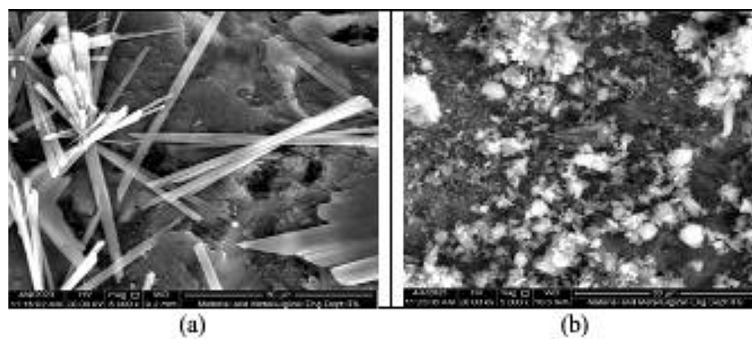


Figure 10. Morphology of green sand (5000×): (a) before adsorption, (b) after adsorption

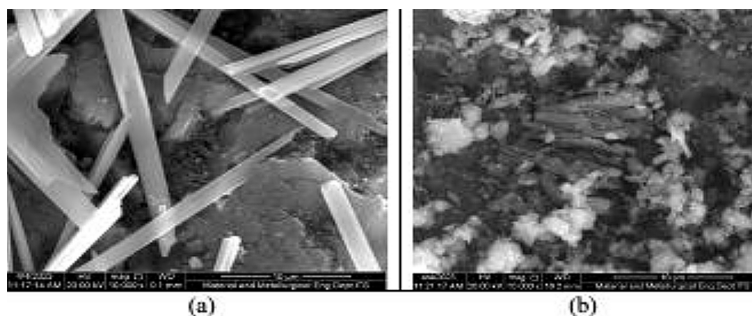
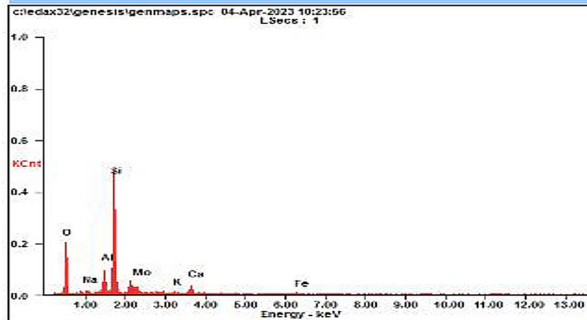


Figure 11. Morphology of green sand (10000×): (a) before adsorption, (b) after adsorption

with a hexagonal structure. Furthermore, based on Figure 12, manganese greensand has a composition of the major element Si (35.87%) and the minor element Na (1.26%). In addition, the material also contains the elements O (35.71%), Al (1.26%), Mo (10.85%), Ca (6.66%), and Fe (1.72%). Furthermore, Figures 10 and 11 show

that the morphology of manganese greensand after the adsorption process contains lump-shaped and white particles, which causes its crystallinity to decrease. The particles are considered quartz minerals mixed with other minerals with rhombohedral and hexagonal structural systems. Furthermore, based on Figure 13, manganese greensand,



Element	Wt%	At%
OK	40.02	57.37
NaK	01.42	01.42
AlK	07.06	06.00
SiK	35.58	29.06
MoL	08.39	02.01
KK	01.17	00.69
CaK	05.24	03.00
FeK	01.12	00.46
Matrix	Correction	ZAF

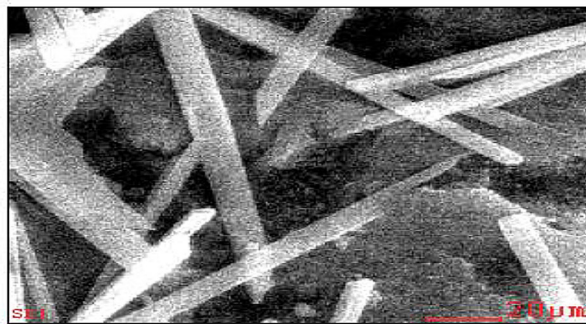
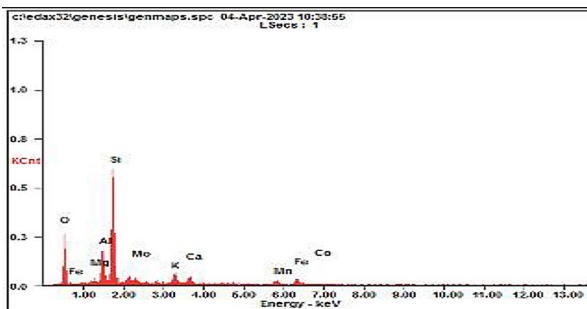


Figure 12. Elemental composition in green sand before adsorption



Element	Wt%	At%
OK	31.79	49.51
MgK	01.37	01.41
AlK	09.24	08.53
SiK	32.42	28.76
MoL	04.95	01.29
KK	04.40	02.80
CaK	03.62	02.25
MnK	04.46	02.02
FeK	06.72	03.00
CoK	01.03	00.44
Matrix	Correction	ZAF

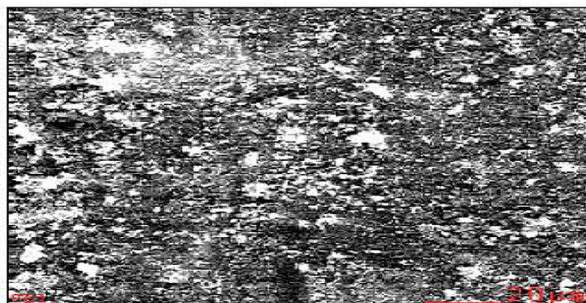


Figure 13. Elemental composition in greensand after adsorption

after adsorption of Fe and Mn, has a major element composition of Si (30.75%) and a minor element of Co (1.22%). In addition, the material also contains the elements O (30.68%), Mg (1.53%), Al (9.59%), Mo (5.75%), K (5.18%), Ca (3.37%), Mn (4.39%), and Fe (7.55%). The increase in the composition of Fe and Mn in the adsorber after the adsorption process indicated that the manganese green sand absorbed the adsorbate Fe and Mn. The adsorption process also did not involve a change in the surface phase of the manganese green sand (MnO_2) and only involved the adsorption process. In addition to Mn^{4+} ions, Mn^{7+} can also be used to coat greensand and can even precipitate stronger metal ions (Outram et al., 2018). Furthermore, Mn^{2+} ions in the adsorbed wastewater have the potential to be extracted and used economically (Nkele et al., 2022).

CONCLUSIONS

Acid mine water treatment using green sand minerals can adsorb Fe metal ions up to 69.94% and Mn metal ions up to 70.61%. The adsorption capacity of Fe and Mn increases along with the concentration of Fe and Mn in acid mine water. The isothermal adsorption model of Fe by greensand minerals following the Freundlich equation test yielded a constant R^2 of 0.9862, n 0.6912, KB 0.2180 mg/g, while the Langmuir equation test resulted in a constant R^2 of 0.8836, b 0.0051 L/mg, q_m 169.4915 mg/g. Meanwhile, the isothermal adsorption model of Mn by greensand minerals followed the Freundlich equation test, resulting in a constant R^2 of 0.9923, n 0.8651, KB 1.0444 mg/g, while the Langmuir equation test resulted in a constant R^2 of 0.6615, b 0.001 L/mg, q_m 500 mg/g. The results of the SEM-EDX test showed that the surface of the greensand mineral was in the form of needle-shaped particles with a hexagonal structure with homogeneous particle shapes before the adsorption of Fe and Mn, whereas after adsorption of Fe and Mn, the particles became inhomogeneous, some clumped like cotton and some in the form of rods.

REFERENCES

1. Budianto, A., Kusdarini, E., Amrullah, N.H., Ningsih, E., Udyani, K.A. 2021. Physics and chemical activation to produce activated carbon from empty palm oil bunches waste. IOP Conference Series: Materials Science and Engineering. IOP Publishing.

2. Basu, S., Ghosh, G., Saha, S. 2018. Adsorption characteristics of phosphoric acid induced activation of bio-carbon: Equilibrium, kinetics, thermodynamics and batch adsorber design. *Process Safety and Environmental Protection*, 117, 125–142. <https://doi.org/https://doi.org/10.1016/j.psep.2018.04.015>
3. Belle, G., Fossey, A., Esterhuizen, L., Moodley, R. 2021. Contamination of groundwater by potential harmful elements from gold mine tailings and the implications to human health: A case study in Welkom and Virginia, Free State Province, South Africa. *Groundwater for Sustainable Development*, 12. <https://doi.org/https://doi.org/10.1016/j.gsd.2020.100507>
4. Budianto, A., Kusdarini, E., Mangkurat, W., Nurdi-ana, E., Asri, N. 2021. Activated Carbon Producing from Young Coconut Coir and Shells to Meet Activated Carbon Needs in Water Purification Process. *Journal of Physics: Conference Series*. Surabaya: IOP Publishing.
5. Budianto, A., Kusdarini, E., Effendi, S., Aziz, M. 2019. The Production of Activated Carbon from Indonesian Mangrove Charcoal. *Materials Science and Engineering*, 462, 1–8. <https://doi.org/10.1088/1757-899X/462/1/012006>
6. Budianto, A., Pratiwi, A.G., Ningsih, S.A., Kusdarini, E. 2023. Reduction of Ammonia Nitrogen and Chemical Oxygen Demand of Fertilizer Industry Liquid Waste by Coconut Shell Activated Carbon in Batch and Continuous Systems. *Journal of Ecological Engineering*, 24(7), 156–164. <https://doi.org/https://doi.org/10.12911/22998993/164759>
7. Galangashi, M.A., Kojidi, S.F.M., Pendashteh, A., Souraki, B.A., Mirroshandel, A.A. 2021. Removing Iron, Manganese and Ammonium Ions from Water Using Greensand in Fluidized Bed Process. *Journal of Water Process Engineering*, 39. <https://doi.org/https://doi.org/10.1016/j.jwpe.2020.101714>
8. Gautama, P.D.I.R.S. 2019. Pembentukan, Pengendalian dan Pengelolaan Air Asam Tambang (II). Bandung: ITB Press.
9. Jung, Y.Y., Choi, S.H., Choi, M., Bong, Y.S., Park, M.Y., Lee, K.S., Shin, W.J. 2023. Acid mine drainage and smelter-derived sources affecting water geochemistry in the upper Nakdong River, South Korea Author. *Science of The Total Environment*, 880. <https://doi.org/https://doi.org/10.1016/j.scitotenv.2023.163353>
10. Kusdarini, E., Budianto, A. 2018. Removal of Manganese from Well-Water on Pasuruan, East Java, Indonesia Using Fixed Bed Cation Exchanger and Prediction of Kinetics Adsorption. *Indian Journal of Science and Technology*, 11(23), 1–7.
11. Kusdarini, E., Budianto, A. 2022. Characteristics and Adsorption Test of Activated Carbon from Indonesian Bituminous Coal. *Journal of Ecological*

- Engineering, 23(10), 1–15. <https://doi.org/https://doi.org/10.12911/22998993/152343>
12. Kusdarini, E., Budianto, A., Gingga, F. 2018. Recovery of Gold with AgNO_3 Pretreatment by Cyanidation at Heap Leaching Cijiwa Gold Ore Processing. *Makara Journal of Science*, 22(2), 77–81.
 13. Kusdarini, E., Hakim, L., Yanuwidi, B., Suyadi, S. 2021. Study in the Development of Fixed Bed Filter Adoption of Public Health of Lake Water Users. *Walailak Journal of Science and Technology*, 18(8), 1–10. <https://doi.org/https://doi.org/10.48048/wjst.2021.9131>
 14. Kusdarini, E., Pradana, D.R., Budianto, A. 2022. Production of Activated Carbon from High-Grade Bituminous Coal to Removal Cr(VI). *Reaktor*, 22(1), 14–20. <https://doi.org/https://doi.org/10.14710/reaktor.22.1.14-20>
 15. Kusdarini, E., Purwaningsih, D.Y., Budianto, A. 2018. Adsorption of Pb^{2+} Ion in Water Well with Amberlite Ir 120 Na Resin. *Pollution Research*, 37(4), 307–312.
 16. Kusdarini, E., Purwaningsih, D.Y., Budianto, A. 2021. Removal Pb^{2+} of Well Water using Purolite C-100 Resin and Adsorption Kinetic. *Pollution Research*, 40(2).
 17. Kusdarini, E., Purwaningsih, D.Y., Iqbal, M. 2017. Removal Pb (II) dari Air Sumur di Kota Pasuruan Menggunakan Proses Cation Exchanger. *Seminar Nasional Sains dan Teknologi Terapan V*, D-39-D-44.
 18. Kusdarini, E., Suyadi, S., Yanuwiyadi, B., Hakim, L. 2019. Model of People's Perception of Water Treatment Equipment: Preliminary Study of the Lake Water Treatment Plan in Gresik Dry Land Area, Indonesia. In: G.T.I. Tawakkal, W. Wike, N. Harahab, A. Utaminingsih, A.S. Leksono (Eds.), *Proceedings of the 13th International Interdisciplinary Studies Seminar* (pp. 1–9). <https://doi.org/10.4108/eai.23-10-2019.2293013>
 19. Kusdarini, E., Yanuwidi, B., Hakim, L., Suyadi, S. 2020. Adoption Model of Water Filter by The Society of Lake Water Users in Dry Land Area, Gresik, East Java, Indonesia. *International Journal on Advanced Science Engineering Information Technology*, 10(5), 2089–2096.
 20. Nkele, K., Mpenyana-Monyatsi, L., Masindi, V. 2022. Challenges, advances and sustainabilities on the removal and recovery of manganese from wastewater: A review. *Journal of Cleaner Production*, 377. <https://doi.org/https://doi.org/10.1016/j.jclepro.2022.134152>
 21. Nowruzzi, R., Heydari, M., Javanbakht, V. 2020. Synthesis of a chitosan/polyvinyl alcohol/activate carbon biocomposite for removal of hexavalent chromium from aqueous solution. *International Journal of Biological Macromolecules*, 147, 209–216.
 22. Ogugua, U.V., Kanu, S.A., Ntushelo, K. 2022. Gibberellic acid improves growth and reduces heavy metal accumulation: A case study in tomato (*Solanum lycopersicum* L.) seedlings exposed to acid mine water. *Heliyon*, (12). <https://doi.org/https://doi.org/10.1016/j.heliyon.2022.e12399>
 23. Outram, J.G., Couperthwaite, S.J., Millar, G.J. 2017. Ferrous poisoning of surface MnO_2 during manganese greensand operation Author links open overlay panel. *Journal of Environmental Chemical Engineering*, 5(3), 3033–3043. <https://doi.org/https://doi.org/10.1016/j.jece.2017.06.006>
 24. Outram, J.G., Couperthwaite, S.J., & Millar, G.J. 2018. Investigation of manganese greensand activation by various oxidants. *Journal of Environmental Chemical Engineering*, 6(4), 4130–4143. <https://doi.org/https://doi.org/10.1016/j.jece.2018.05.060>
 25. Tehrani, G.F., Rubinos, D.A., Kelm, U., Ghadimi, S. 2023. Environmental and human health risks of potentially harmful elements in mining-impacted soils: A case study of the Angouran Zn–Pb Mine, Iran. *Journal of Environmental Management*, 334. <https://doi.org/https://doi.org/10.1016/j.jenvman.2023.117470>